The role of the cooperative Jahn–Teller effect in the charge-ordered $La_{1-x}Ca_xMnO_3$ $(0.5 \leqslant x \leqslant 0.87)$ manganites

R. K. Zheng, G. Li, A. N. Tang, Y. Yang, W. Wang, and X. G. Li[a)]
Structure Research Laboratory, Department of Materials Science and Engineering, University of Science and Technology of China, Anhui, Hefei 230026, China

Z. D. Wang
Structure Research Laboratory, Department of Materials Science and Engineering, University of Science and Technology of China, Anhui, Hefei 230026, China and Department of Physics, The University of Hong Kong, Hong Kong, China

H. C. Ku
Department of Physics, The National Tsinghua University, Hsinchu 300, Taiwan, China

(Received 2 September 2003; accepted 27 October 2003)

Based on the magnetoresistance, magnetization, ultrasound, and crystallographic data, we studied the role of the cooperative Jahn–Teller (JT) effect in the charge-ordered (CO) state for $La_{1-x}Ca_xMnO_3$. We found that, with increasing the fraction of Q_3 mode of JT distortion and decreasing that of Q_2 mode in the CO state, the magnetic structure evolves from charge-exchange-type to C-type and the orbital ordering changes from $3d_{x^2-r^2}/3d_{y^2-r^2}$-type to $3d_{z^2-r^2}$-type, with the strength of ferromagnetism and the phase separation tendency being suppressed. At the same time, the stability of the CO state and the cooperative JT lattice distortion increase. These effects imply that the cooperative JT effect with different vibration modes is the key ingredient in understanding the essential physics of the CO state. © *2003 American Institute of Physics.* [DOI: 10.1063/1.1635662]

The charge, spin, and orbital orderings in manganites have recently attracted much attention because of their intriguing electronic, magnetic, and structural properties.[1,2] As a typical example of charge ordering cases, the $La_{1-x}Ca_xMnO_3$ system with the doping range of $0.5 \leqslant x \leqslant 0.875$, especially for a commensurate fraction of doping level such as $x=1/2$, 2/3, 3/4, undergoes evident charge-, spin-, and orbital-ordering phase transitions upon cooling below the charge-ordering transition temperature T_{CO}.[3,4] In the charge-ordered (CO) state, the ordering of Mn^{3+} and Mn^{4+} species within the MnO_2 plane leads to exotic static stripe phase with insulator antiferromagnetic ground state.[3,5] Upon increasing x from 0.5 to 0.75 the magnetic structure evolves gradually from charge-exchange (CE)-type to C-type, and is almost C-type for $x>0.75$,[6] with the strength of ferromagnetism and phase separation tendency being suppressed.[7,8] At the same time, the magnitude of the cooperative Jahn–Teller (JT) distortion and the robustness of the CO state increase.[9] Moreover, the crystal structure in the CO state changes from tetragonally compressed orthorhombic ($b/\sqrt{2}<a\approx c$ for $x<0.75$) to tetragonally elongated orthorhombic ($c\approx a<b/\sqrt{2}$ for $x>0.75$) near $x=0.75$.[10] For $x>0.75$, both the JT distortion and the stability of CO state decrease with increasing doping level x. Although theoretical and experimental studies have indicated that the magnetic, transport, and crystallographic properties, the phase separation, and the electron–lattice interaction in manganites are closely related to the JT effect,[2,11–14] an *overall* profound understanding of the key role of the JT effect in the CO state and detailed explanations for the observed experimental results are still incomplete.

In this letter, we *experimentally* elucidate the relationships of the cooperative JT effect having different vibration modes with a variety of factors in $La_{1-x}Ca_xMnO_3$, such as evolutions of magnetic and crystal structures, orbital ordering, the stability of the CO state, the strength of ferromagnetism, the phase separation tendency, the magnitude of the lattice distortion. The analyses of the experimental data suggest that the cooperative JT effect with different vibration mode plays a key role in understanding the rich physics of the CO state.

The $La_{1-x}Ca_xMnO_3$ samples were synthesized via a coprecipitation method. Resistivity $\rho(T)$ was measured using a standard four-probe technique in magnetic fields up to 14 T. Magnetizations were measured at $H=0.1$ and 5 T using a Quantum Design superconducting quantum interference device magnetometer. The longitudinal ultrasound was measured using the Matec-7700 series ultrasonic equipment using a pulse-echo-overlap technique.

Based on our previous systematic resistivity data measured under magnetic fields up to 14 T for $La_{1-x}Ca_xMnO_3$ $(0.5 \leqslant x \leqslant 0.9)$[9] series, we analyze the magnetoresistance $[MR=(\rho_0-\rho_H)/\rho_H]$ effect under a field of 14 T at 75 K for different doping levels. The x-dependence of the MR effect is plotted in Fig. 1(a). The change of T_{CO} induced by the field (14 T) [that is, $\Delta T_{CO}=T_{CO}(0\ T)-T_{CO}(14\ T)$], is also plotted against x in the inset of Fig. 1(a). It is seen that the MR effect decreases rapidly from the order of 10^5 to nearly zero upon increasing x from 0.5 to 0.75, while it increases slightly upon further increasing x

a)Electronic mail: Lixg@ustc.edu.cn

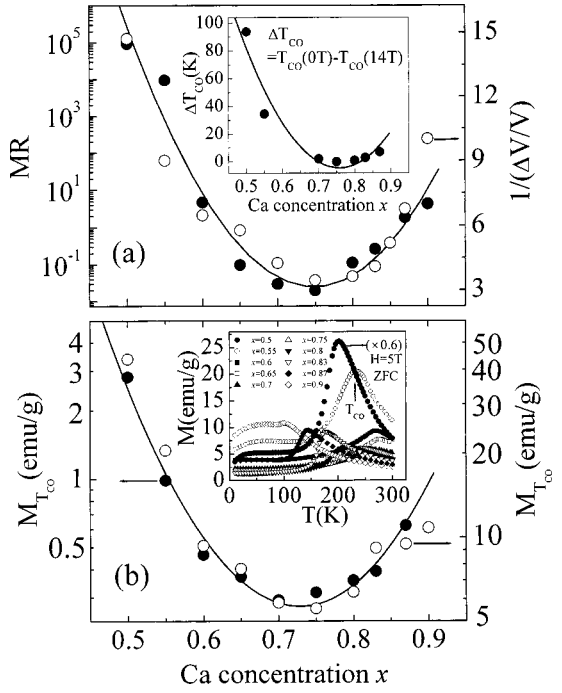

FIG. 1. (a) The MR effect at $T=75$ K and $H=14$ T as a function of doping level x for $La_{1-x}Ca_xMnO_3$. The solid line is a guide to the eyes. The open circles are the $1/\Delta V/V$ versus x data. Inset in (a) is the x-dependence of the magnetic field (14 T) induced change of the ΔT_{CO}. (b) The magnetization at $T_{CO}(M_{T_{CO}})$ measured at $H=0.1$ and 5 T as a function of doping level x, the solid line is a guide to the eyes for $H=0.1$ T, the open circles are the $M_{T_{CO}}$ versus x data measured at $H=5$ T. Inset in (b) is the temperature dependence of the zero-field-cooled magnetization for $La_{1-x}Ca_xMnO_3$.

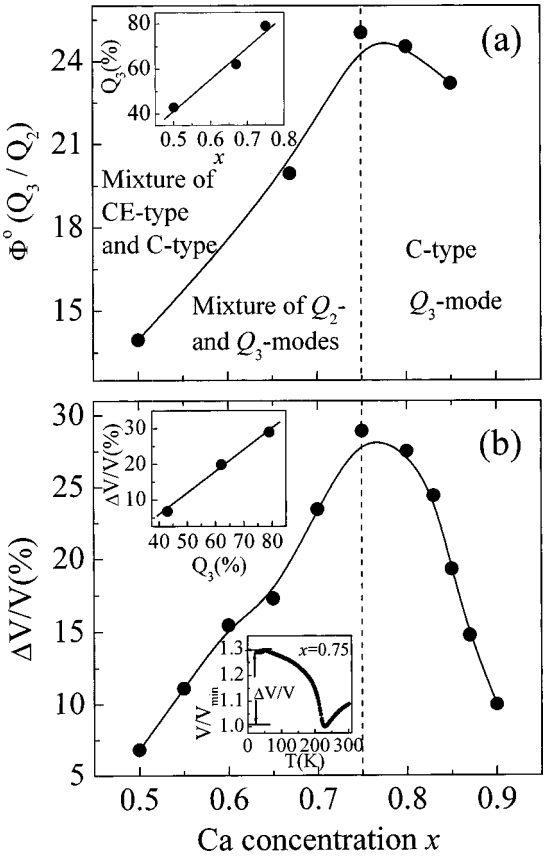

FIG. 2. (a) Variation of the JT vibration anisotropy Φ as a function of doping level x. The inset in (a) is the x-dependence of the fraction of the Q_3 mode. (b) Variation of the relative change of the ultrasound ($\Delta V/V$) as a function of doping level x. The solid line is a guide to the eyes. The inset (upper) in (b) is the $\Delta V/V$ versus Q_3% curve. The inset (lower) in (b) is a typical temperature dependence of the ultrasound for $La_{1-x}Ca_xMnO_3$.

from 0.75 to 0.87. The x-dependence of ΔT_{CO} shows a behavior very similar to that of the MR. These magnetic-field effects on MR and ΔT_{CO} demonstrate that the CO state becomes increasingly robust as x increases from 0.5 to 0.75, and appears to be the most robust at (or near) $x=0.75$. One may naturally think that these magnetic-field effects on MR and ΔT_{CO} may relate to the intrinsic strength of the ferromagnetism of the system. To clarify this point, we measured the temperature dependence of the magnetization at $H=0.1$ and 5 T for $La_{1-x}Ca_xMnO_3$ series. As shown in the inset of Fig. 1(b), the magnetization shows a peak at T_{CO}, and decreases prominently with the development of charge and orbital ordering state. It is interesting to find that the magnetization at T_{CO} (i.e., $M_{T_{CO}}$) is the largest for $x=0.5$, and decreases rapidly upon increasing x from 0.5 to 0.75, reaching the minimum at $x\approx0.75$. When x increases from 0.75 to 0.9, the $M_{T_{CO}}$ increases slightly. By comparing the x-dependences of the MR and the ΔT_{CO} with that of the $M_{T_{CO}}$, it is straightforward to conclude that the decrease of the MR and the ΔT_{CO} with increasing x is due to the decrease of intrinsic strength of the ferromagnetism of the system. However, what drives the system into a less ferromagnetic state as x increases from 0.5 to 0.75?

It has been shown that the ratio of the JT vibration mode Q_3/Q_2 in a given static distortion is[15–17]

$$\tan\Phi=\frac{(2/\sqrt{6})(2m-l-s)}{\pm(2/\sqrt{2})(l-s)}, \tag{1}$$

where s and l are the short and long Mn–O bond lengths, respectively, pointing along the [100] and [010] axes, alternatively, m is the bond length along the [001] axis, $s\leqslant m\leqslant l$, and Φ is the angle between the state vectors and the Q_2 axis, which measures the relative fractions of Q_3 and Q_2 modes. In the high-anisotropy limit ($m=s$), only the Q_3 mode is present, corresponding to $\Phi=30°$; while for the low-anisotropy case ($\Phi=0°$), there is only Q_2 mode.[17] In fact, in real JT distorted materials, both the Q_2 and Q_3 modes contribute to the lattice distortion; nevertheless, the ratio Q_3/Q_2 depends on the value of l, m, and s. Using the Mn–O bond length obtained from low-temperature, high-resolution neutron diffraction measurements for $La_{0.5}Ca_{0.5}MnO_3$,[5] $La_{0.33}Ca_{0.67}MnO_3$,[18] $La_{1-x}Ca_xMnO_3$ ($x=0.8,0.85$),[19] and the Mn–O bond length at 70 K obtained from Rietveld analysis of our high resolution powder x-ray diffraction data for $x=0.75$ ($R_P=8.14\%$, $R_{WP}=11.4\%$, $\chi^2=1.74$), we calculated the Φ using Eq. (1).

The x-dependence of the Φ is plotted in Fig. 2(a). It is seen that, for $x=0.5$, $\Phi=13.5°$, indicating a modest anisotropy. Interestingly, when x increases from 0.5 to 0.75, the Φ increases almost linearly and evolves toward the high-anisotropy limit ($\Phi=24.53°$ for $x=0.75$). The increase of Φ suggests a growth of Q_3 mode and a decrease of Q_2 mode. With further increase of x from 0.75, the Φ decreases slightly, but it remains at a high value, indicating that the Q_3 is the predominant mode for $x>0.75$. If we assume that the fraction of Q_3 mode in the high-anisotropy limit (i.e.,

$\Phi=30°$, corresponding to pure Q_3 mode) is 1, then the fraction of Q_3 mode in the CO state at a fixed doping level x can be calculated as

$$Q_3\% = \frac{\tan\Phi°}{\tan 30°}, \tag{2}$$

Following this equation, we obtained the x-dependence of the fraction of Q_3, as shown in the inset of Fig. 2(a). The $Q_3\% \sim x$ relationship clearly demonstrates that the fraction of Q_3 mode increases almost linearly with increasing doping level x. As we recently reported, the relative change of the ultrasound (i.e., the $\Delta V/V$), reflecting the magnitude of the cooperative JT distortion in the CO state, also increases almost linearly upon increasing doping level from $x=0.5$ to $x=0.75$.[9] The $\Delta V/V$ versus x curve is shown in Fig. 2(b). It is, therefore, very possible that the increase of the cooperative JT distortion (or equivalently, the $\Delta V/V$) upon increasing x can be intrinsically related to the increase of the fraction of Q_3 mode. To further look into this issue, we plot the $\Delta V/V$ as a function of $Q_3\%$, as shown in the inset of Fig. 2(b). The $\Delta V/V$ increases almost linearly with the increase of the fraction of Q_3, which strongly suggests that the increase of the $\Delta V/V$ is microscopically due to the growth of Q_3-mode JT distortion and decrease of Q_2 mode, and moreover, demonstrates that the cooperative JT distortion contributed from Q_3 mode is much more prominent than that contributed from Q_2 mode.

It is worth noting that the neutron diffraction measurements on $La_{1-x}Ca_xMnO_3$ $(0.5 \leqslant x \leqslant 1)$ have shown that the magnetic structure in the ground state for $x=0.5$ is CE-type, while it is C-type for $x>0.75$.[6] For $0.5<x<0.75$, the magnetic structure is a mixture of the two types, and the C-type magnetic structure grows at the cost of the CE-type's decline upon increasing x from 0.5 to 0.75.[6] As pointed out in Refs. 2 and 11–14, the CE-type magnetic structure originates from $3d_{x^2-r^2}/3d_{y^2-r^2}$ orbital ordering, consistent with Q_2-mode cooperative JT distortion, and the C-type magnetic structure originates from $3d_{z^2-r^2}$ orbital ordering, consistent with Q_3-mode cooperative JT distortion. Based on this scenario, one can conclude that the growth of C-type magnetic structure with increasing x is the result of the increase of the fraction of Q_3-mode cooperative JT distortion, corresponding to the evolution of the orbital ordering from $3d_{x^2-r^2}/3d_{y^2-r^2}$ to $3d_{z^2-r^2}$. From this picture, the phase separation tendency and the magnetic-field effects on the stability of the CO state can readily be understood as follows: upon increasing x from 0.5 to 0.75 the strength of the electron–lattice interaction with the cooperative JT distortion and the fraction of C-type magnetic structure increase because of the increase of the fraction of the Q_3-mode JT distortion. Hence, the strength of the ferromagnetism of the system was suppressed, and thus the phase separation tendency decreases. On the other hand, it is natural to expect that the magnetic-field effects on the stability of CO state will become less effective because the ferromagnetism of the system decreases in the presence of more and more C-type magnetic structure. In fact, the cooperative JT effect with different vibration mode on the stability of CO state (or MR) can be more intuitively understood if we plot the $1/\Delta V/V$ as a function of doping level x in Fig. 1(a). The JT effect with different vibration mode effects on the magnetism is also observed for low-doped $R_{2/3}D_{1/3}MnO_3$ (R=La, Tb, La-Pr, Pr, La-Y, D=Ca, Sr) manganites, in which a low magnetic moment is always associated with the predominance of Q_3-mode JT distortion and a high magnetic moment with Q_2 mode.[17]

In summary, we have studied the role of cooperative Jahn-Teller effect in the CO state for $La_{1-x}Ca_xMnO_3$. The evolutions of magnetic structure from CE-type to C-type, the orbital ordering from $3d_{x^2-r^2}/3d_{y^2-r^2}$ to $3d_{z^2-r^2}$, and crystal structure from tetragonally compressed to tetragonally elongated orthorhombic, the suppression of ferromagnetism and phase separation tendency, the increase of the robustness of the CO state, the increase of the magnitude of the cooperative JT lattice distortion can all be attributed to the increase of the relative fraction of Q_3-mode JT distortion with respect to Q_2 mode. These results suggest that the cooperative JT effect with different vibration modes plays an essential role of physics in the CO state for the $La_{1-x}Ca_xMnO_3$ system.

This work was supported by the Chinese National Nature Science Fund, and the Ministry of Science and Technology of China.

[1] C. Martin, A. Maignan, M. Hervieu, and B. Raveau, Phys. Rev. B **60**, 12191 (1999).
[2] T. Hotta, A. L. Malvezzi, and E. Dagotto, Phys. Rev. B **62**, 9432 (2000).
[3] S. Mori, C. H. Chen, and S.-W. Cheong, Nature (London) **392**, 473 (1998).
[4] A. P. Ramirez, P. Schiffer, S.-W. Cheong, C. H. Chen, W. Bao, T. T. M. Palstra, P. L. Gammel, D. J. Bishop, and B. Zegarski, Phys. Rev. Lett. **76**, 3188 (1996).
[5] P. G. Radaelli, D. E. Cox, M. Marezio, S.-W. Cheong, P. E. Schiffer, and A. P. Ramirez, Phys. Rev. Lett. **75**, 4488 (1995).
[6] E. O. Wollan and W. C. Koehler, Phys. Rev. **100**, 545 (1955).
[7] S. W. Cheong and H. Hwang, in *Colossal Magnetoresistance Oxides*, edited by Y. Tokura (Gordon and Breach, New York, 2000), pp. 237–280.
[8] H. D. Zhou, G. Li, S. J. Feng, Y. Liu, T. Qian, X. J. Fan, and X. G. Li, Solid State Commun. **122**, 507 (2002).
[9] X. G. Li, R. K. Zheng, G. Li, H. D. Zhou, R. X. Huang, J. Q. Xie, and Z. D. Wang, Europhys. Lett. **60**, 670 (2002).
[10] R. K. Zheng, R. X. Huang, A. N. Tang, G. Li, X. G. Li, J. N. Wei, J. P. Shui, and Z. Yao, Appl. Phys. Lett. **81**, 3834 (2002).
[11] T. Mizokawa and A. Fujimori, Phys. Rev. B **56**, R493 (1997).
[12] M. Capone, D. Feinberg, and M. Grilli, Eur. Phys. J. B **17**, 103 (2000).
[13] E. Dagotto, T. Hotta, and A. Moreo, Phys. Rep. **344**, 1 (2001).
[14] D. I. Khomskii and K. I. Kugel, Phys. Rev. B **67**, 134401 (2003).
[15] J. Kanamori, J. Appl. Phys. **31**, 14S (1960).
[16] J. B. Goodenough, A. Wold, R. J. Arnott, and N. Menyuk, Phys. Rev. **124**, 373 (1961).
[17] F. Rivadulla, A. A. López-Quintela, J. Mira, and J. Rivas, Phys. Rev. B **64**, 052403 (2001).
[18] P. G. Radaelli, D. E. Cox, L. Capogna, S.-W. Cheong, and M. Marezio, Phys. Rev. B **59**, 14440 (1999).
[19] M. Pissas, G. Kallias, M. Hofmann, and D. M. Többens, Phys. Rev. B **65**, 064413 (2002).